MEGA JOURNAL OF CASE REPORTS

Research Article

Compiled Date: April 08, 2023

Integration of Spatial Transcriptome and Single-Cell Sequencing to Identify Specific Gene Expression in Spatially Organized Regions and Crosstalk between Tumor Microenvironments in Patients with Lung Squamous Cell Carcinoma Combined with Non-alcoholic Fatty Liver Disease

Hang Yang* **and Qi Nian Jiang**

Guizhou Medical University, Guiyang, 550004, China

***Corresponding author**: Hang Yang, Guizhou Medical University. No.9 Beijing Road, Yunyan District, Guiyang of Guizhou 550004, China, Tel: +86-17716657899; E-mail: hangyang1999@163.com

Abstract

Background: Non-alcoholic fatty liver disease (NAFLD) is a common type of liver disease and is showing a high prevalence worldwide. The liver fibrosis caused by NAFLD increase the risk of extrahepatic diseases. Lung cancer is one of the most common cancers causing death in the world, with lung squamous cell carcinoma (LUSC) as its main tissue type. Previous clinical cohort studies suggest NAFLD as a risk factor for lung cancer, but the exact mechanism is unclear.

Aims: to explore the shared genes between NAFLD and LUSC from the transcriptome with bioinformatics methods, and to verify the in-situ expression of our genes and the relationship and communication with cells.

Methods: First, we use weighted gene co-expression network analysis (WGCNA) and Deseq2 analysis to identify the differentially expressed core intersection genes driving the disease; second, we construct a PPI reciprocal network to identify hub genes; then perform prognostic and immune analysis at the bulk-RNA level, use single-cell sequencing datasets to validate our findings on subdivided cell subpopulations, then use spatial transcriptome datasets to explain the in situ expression of our hub genes; finally, we construct a ceRNA regulatory network to demonstrate the reciprocal relationships between molecules.

Results: We identified 11 genes that drive disease progression in patients with NAFLD and LUSC, GO and KEGG revealing their involvement in cancer first-off pathways, and immune and prognostic analyses revealing that our TOP3 (BRCA1, CAV1, CDKN1A) genes are associated with prognosis and immune cells. Single cell analysis results demonstrate that our genes are highly expressed in malignant and stromal cells and involved in

cell-to-cell interactions, where spatial transcriptome analysis results show that our gene set scores are highly expressed in malignant and cancer-associated cells, and imaging results also demonstrate that the core gene CDKN1A is highly expressed in basal cells (tumor cells). The final regulatory network demonstrates the regulatory network between miRNA-lncRNA-Hub gene.

Conclusions: our work identifies the function of shared genes CDKN1A, BRCA1, and CAV1 in squamous lung cancer, such as those between NAFLD and LUSC. In this investigation, novel markers for squamous lung cancer identified in this investigation.

Keywords: Multidimensional integrated analysis; Non-alcoholic fatty liver disease; Spatial transcriptome; CDKN1A; Lung squamous cell carcinoma

Abbreviations NAFLD: Non-Alcoholic Fatty Liver Disease; LUSC: Lung Squamous Cell Carcinoma; TCGA: The Cancer Genome Atlas; HR: Hazard Ratio; GO: Gene Ontology; WGCNA: Weighted Gene Co-Expression Network Analysis

Introduction

Non-Alcoholic Fatty Liver Disease (NAFLD) is a type of liver disease that is linked to insulin resistance, obesity, and the metabolic syndrome **[1].** NAFLD is significantly associated with obesity **[2],** with an estimated frequency of 25% in the NAFLD group and 3% to 5% in Non-Alcoholic Steatohepatitis (NASH) **[1,3,4].** Hepatic steatosis happens when the fat level of hepatocytes surpasses 5%, resulting in cell death, inflammation, and fibrosis, and hence NASH **[5-7].** As NASH worsens, liver fibrosis occurs, causing the liver to stiffen and become functionally compromised **[8].** Furthermore, advanced fibrosis is linked to overall mortality and the individuals with advanced fibrosis dying at three times the risk of people without liver disease. Thus, the fibrosis stage, rather than the steatosis stage, is directly related to total mortality in NAFLD patients **[9].** Lung cancer is a major cause of cancer-related mortality. Non-Small Cell Lung Cancer (NSCLC) accounts for 85% of all lung cancers. The most frequent type of malignant tissue is squamous cell carcinoma of the lung, which accounts for 50% of all NSCLC cases **[10,11].** Squamous lung tumors are frequently seen in the center of the lung, often begin in the proximal bronchi, and are more prone to invade big blood arteries **[12,13].** Mutations for targeted therapy are uncommon in squamous lung cancer patients **[14,15].** As a result, all aspects of a patient's clinical history, disease, and tumor features must be taken into account to guarantee that they are treated effectively and that the patient's prognosis is improved. This is especially crucial in the first-line therapy of individuals with advanced illness **[16,17].** Previous studies have revealed an association between NAFLD and extrahepatic cancers. Results of a cohort study reveal that NAFLD increases patients' risk of developing lung cancer by 30% **[18].** Several studies in large cohorts have also suggested an increased risk of lung cancer in patients with NAFLD (HR, 1.38; 95% CI, 1.03-1.84) **[19,20].** Most of the current studies are mainly clinical studies and few have explored the regulatory mechanisms between these two diseases in terms of molecular mechanisms. Therefore, we use bioinformatics approaches to explore the shared genes between the two starting from the transcriptome, single cell sequencing allows us to better explore the patient's tumor microenvironment **[21],** and spatial transcriptome allows us to understand the in-situ expression of genes **[22],** using single cell combined with spatial transcriptome approaches to verify the in situ expression of our genes and the relationship and communication with cells from different dimensions and precision.

Materials and Methods

Data collection and cleaning

The TCGA database (https://portal.gdc.cancer.gov/) was used to download transcriptome data from LUSC patients (n = 550) in both count and FPKM formats, and we combined clinical data from pertinent tumor and normal samples for in-depth analysis. The dataset of NAFLD expression data was taken from dataset GSE49541 under the Gene Expression Omnibus (GEO) database, which covers 72 samples and patient staging includes advanced (fibrosis stage 3-4) and moderate (fibrosis stage 0-1). We first acquired the expression profiles, then extracted the transcripts with gene type of protein coding as protein coding genes to obtain the protein coding gene expression profiles, and then obtained the transformed expression profiles, and deleted the NA values of the samples, before using the impute.knn function of the R package impute to fill in the missing values. To fill in the missing data, the number of neighbours was set to K = 10. In addition, a log2 transformation was done on the data to create the data matrix for analysis.

Identification of differentially expressed genes and WGCNA analysis

To extract the differential genes between the TCGA tumor group and the normal group, we utilized the R package DESeq2 (Differential gene expression analysis based on the negative binomial distribution) **[23].** In addition, we used the R package limma (linear models for microarray data) to run a difference analysis on the GEO dataset to determine which genes differed between the comparison and control groups for different stage of liver fibrosis **[24].** We did Weighted Gene Co-Expression Network Analysis (WGCNA) **[25]** analysis of the expression profile matrix of patients with LUSC and patients with liver fibrosis using Sanger Box 3.0 **[26]** to find the most relevant modular genes for clinical characteristics. The soft threshold for the TCGA dataset was set to 8 and for the GEO dataset to 6, and we also plotted the connection between clinical and modular genes.

Crossover gene screening and discovery of hub genes

We plotted the WGCNA analysis and the Venn diagram of gene differential expression results using a JavaScript ""jvenn"" script **[27],** and we used the STRING (functional protein association networks) website (https://www.string-db.org/) to construct protein interaction networks of intersecting genes, and we used Cytoscape (https://cytoscape.org/) software to find the TOP3 pivotal genes. We used GO annotations of genes from the R package org for gene set functional enrichment analysis. We used GO annotations of genes from the R package org for gene set functional enrichment analysis.org.Hs.eg.db was utilized as the background set, genes were mapped to the background set, and enrichment analysis was performed using the R package clusterProfiler **[28]** to obtain gene set enrichment results. The lowest gene set was 5, the maximum gene set was 5000, the P value was 0.05, and the FDR was 0.25.

Prognostic and immunological analysis of Hub genes

We plotted KaplanMeier survival curves using the R package survival. In addition, using the R package ESTIMATE **[29],** we computed the stromal score, immunological score, and Estimate score of patients with squamous lung cancer to better understand the tumor microenvironment. We collected clinical data from squamous lung cancer patients, using R software to assess variations in gene expression at different clinical sample phases, did difference analysis between two groups using an unpaired Student's t-test, and compared multiple sample groups using ANOVA. To investigate the link between core genes and immune cells, the EPIC and MCPcount algorithms were utilized **[30,31].**

Analysis of diversity data of hub genes in single cells

We chose the dataset GSE117570 (N = 4) from the TISCH2 [32] website database to input our core genes to investigate the expression of core genes in the tumor microenvironment of lung cancer patients, and performed analyses such as transcription factors and cellular communication. In the supplemental file, we include the differentially expressed genes from the GEO single-cell dataset as well as the META annotation file information (which includes cell type annotations as well as the results of downscaling clustering).

Spatial transcriptome analysis (Sequencing-based)

The 10X GENOMICS website (https://www.10xgenomics.com/cn/resources/datasets/human-lung-cancer-ffpe-2-standard) provided us with the Human Lung Cancer (FFPE) Spatial Gene Expression Dataset by Space Ranger 2.0.0. The supplemental file contains the Spatial Gene Expression Dataset by Space Ranger 2.0.0, which includes the corresponding immunohistochemistry images as well as the corresponding gene expression and location in space. We processed the spatial transcriptomics data with the R package Seurat [33] and visualized it with ggplot2. We normalized the data with the SCTransform function, ran the RunPCA function to reduce the dimensionality, selected 1:15 principal components, and visualized the expression of the core genes at different locations on the sliced tissue with Dimplot.

Finally, we used the AddModuleScore scoring method to map the core genes as gene sets to our spatial transcriptome data, and the cell type clustering of joint single cell and spatial transcriptome inferred spatial transcriptome was mapped using the MIAscoring method [34].

Analysis of spatial datasets (Imaging-based)

We got healthy slices of non-small cell lung cancer tissue from (https://nanostring.com/products), a dataset developed using the Nanostring CosMx Spatial Molecular Imager (SMI), and used the seurat website to display the spatial expression of our Hub genes.

Building CERNA Network

Using the Perl (https://strawberryperl.com/) programming language, we generated text files of the reciprocal network, which we then imported into cytoscape and altered to obtain the ceRNA regulatory network, which included the four core genes and their related miRNAs and lncRNAs. The database files can be found in the supplemental file.

Statistical analysis

All statistical analyses included were done in R language version 4.1.1(https://www.r-project.org/) and P value< 0.05 for different comparisons were considered statistically significant.

Results

Identification of differentially expressed shared genes between patients with NAFLD and lung squamous carcinoma

We obtained the most relevant black module for advanced liver fibrosis in NAFLD patients and the most relevant turquoise module for lung cancer tumor samples using the WGCNA analysis **method (Figure 1B and H). (Figure 1A, C, F and G)** depicts the soft thresholds related with module correlation. We identified the differentially expressed genes that were upregulated and downregulated in the two datasets by examining the differential expression of the two datasets **(Figure 1D and E).**

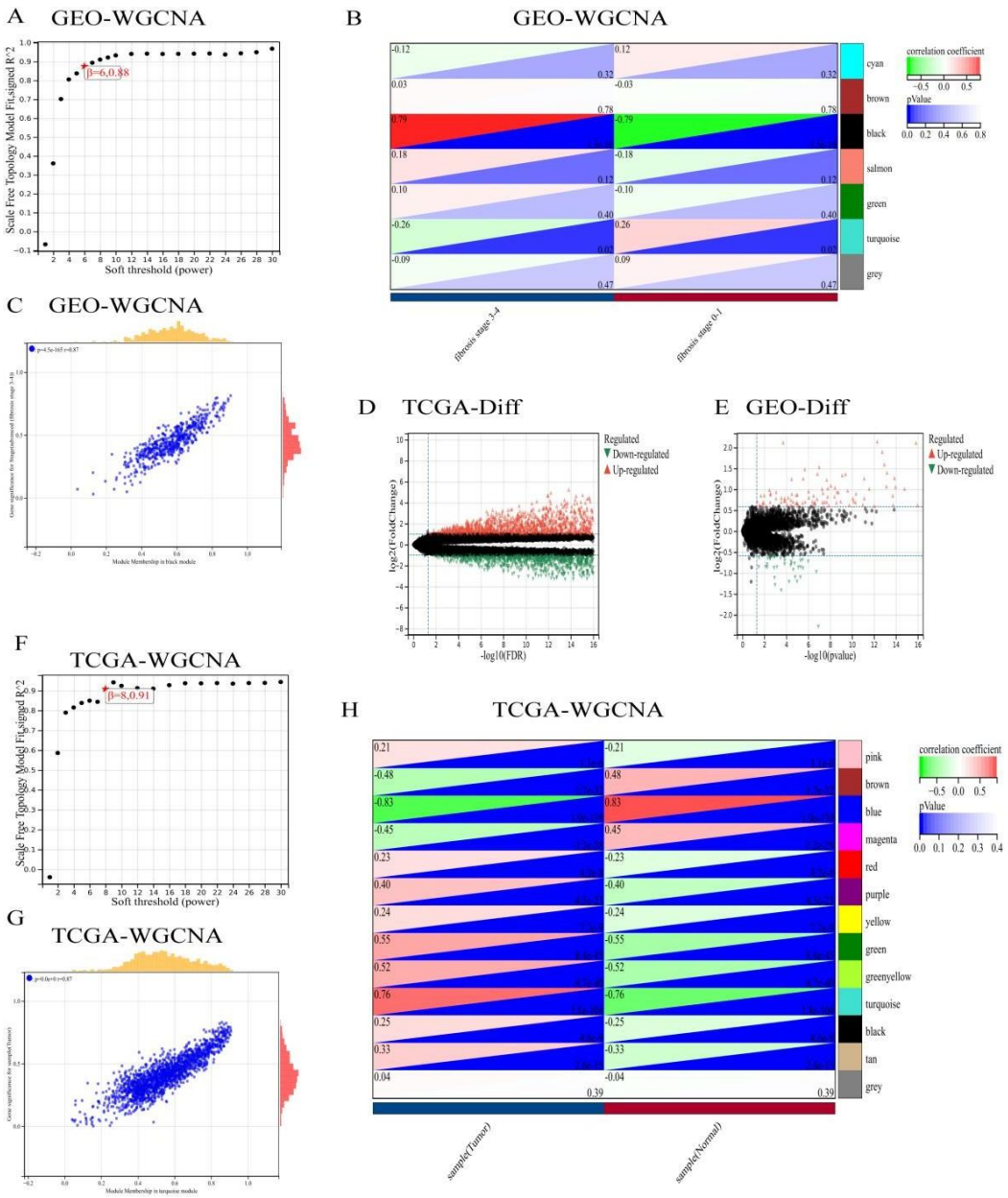

Figure 1: Identification of differentially expressed genes and clinical trait-related module genes. (A, B) WGCNA analysis of GEO dataset with soft thresholding. (C) Correlation of black module with grade of liver fibrosis. (D, E) Identification of differentially expressed genes in GEO and TCGA datasets. (F, H) WGCNA analysis of TCGA dataset with soft thresholding. (G) Correlation of modules with tumor traits.

Identification and biological pathway enrichment analysis of Hub genes

Using Venn diagrams, we found 11 common genes in the two disorders by intersecting the findings of WGCNA and differential expression analyses **(Figure 2A).** The cytoscape software study revealed the hub genes of TO3 by establishing the PPI protein interaction network, with the CDKN1A gene contributing the most to the network **(Figure 2B and C).** We analyzed our data using the GO KEGG approach to elucidate the biological pathways in which our common genes are involved and enriched. GO results showed that most genes were enriched in cell cycle checkpoint **(Figure 2E),** KEGG results were enriched in Focal adhesion, and MicroRNAs in cancer associated pathways **(Figure 2D and F).**

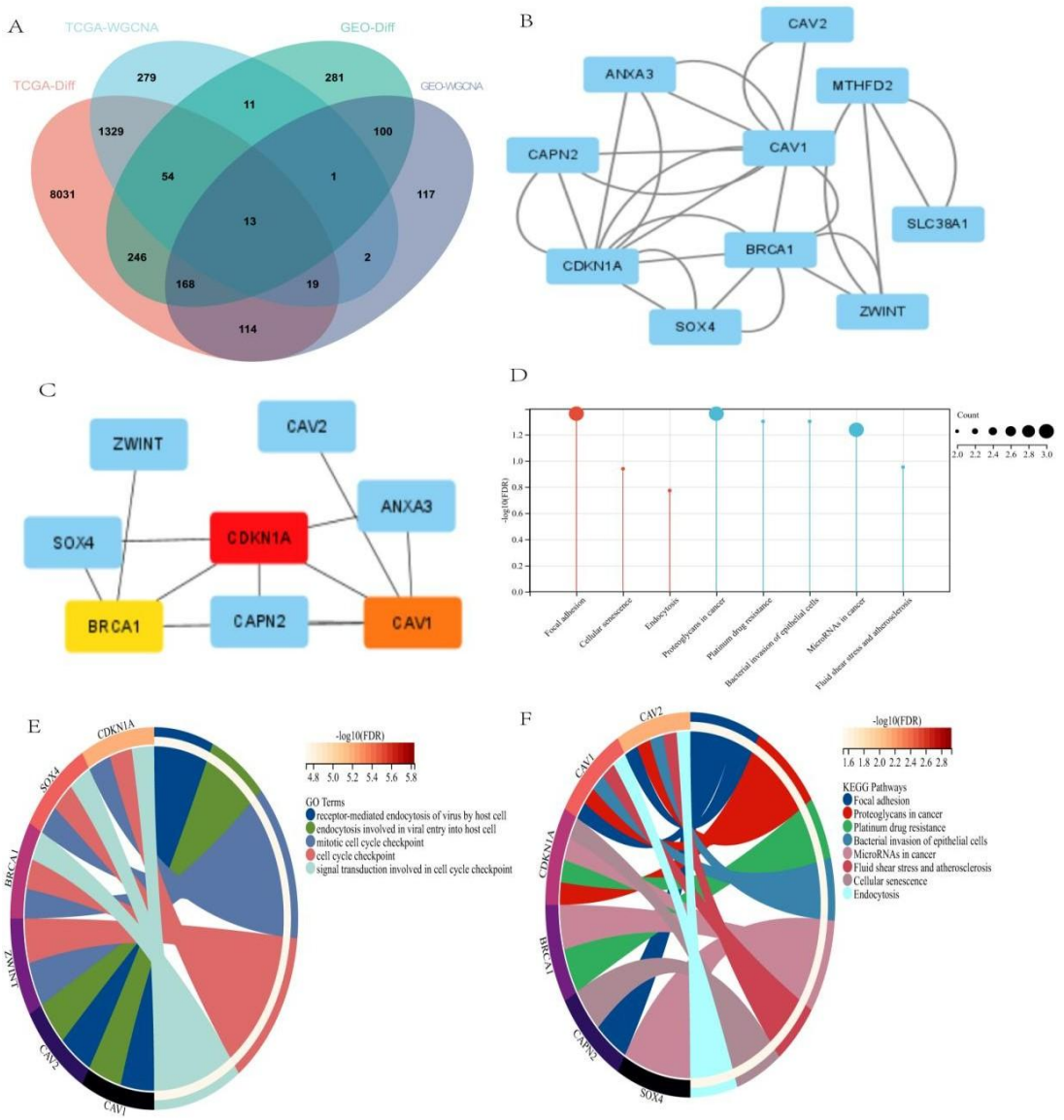

Figure 2: Identification and enrichment analysis of Hub genes. (A) Wayne diagram showing intersection genes. (B, C) Protein Interaction Network of Intersecting Genes. (D, F) KEGG analysis of the enrichment pathway of crossover genes. (E) GO analysis of the enrichment pathway of crossover genes.

Immunological and prognostic correlation analysis of hub genes

The KM curves show the prognosis analysis of core genes, where core genes were important in differentially expressed subgroups, such as CDKN1A, CAV1, and SOX4 **(Figure 3A).** The Estimate method revealed a substantial positive association between CDKN1A expression and matrix and EstimateScore, but not with immunological score **(Figure 3B).** As indicated in the image, Epic and McpCount analyses revealed a favourable link between the CDKN1A gene and immune cells. CDKN1A was most highly correlated with Endothelia cells, CAFS, and CD4 T **(Figure 3C and D).** We also explored the mutational profile of the amino acid structural domain of CDKN1A in relation to the epigenetic modifications M6A, M5C, and M1A **(Figure 3E and H)**. CDKN1A is differentially expressed in clinical samples with different staging T, N **(Figure 3F and G).**

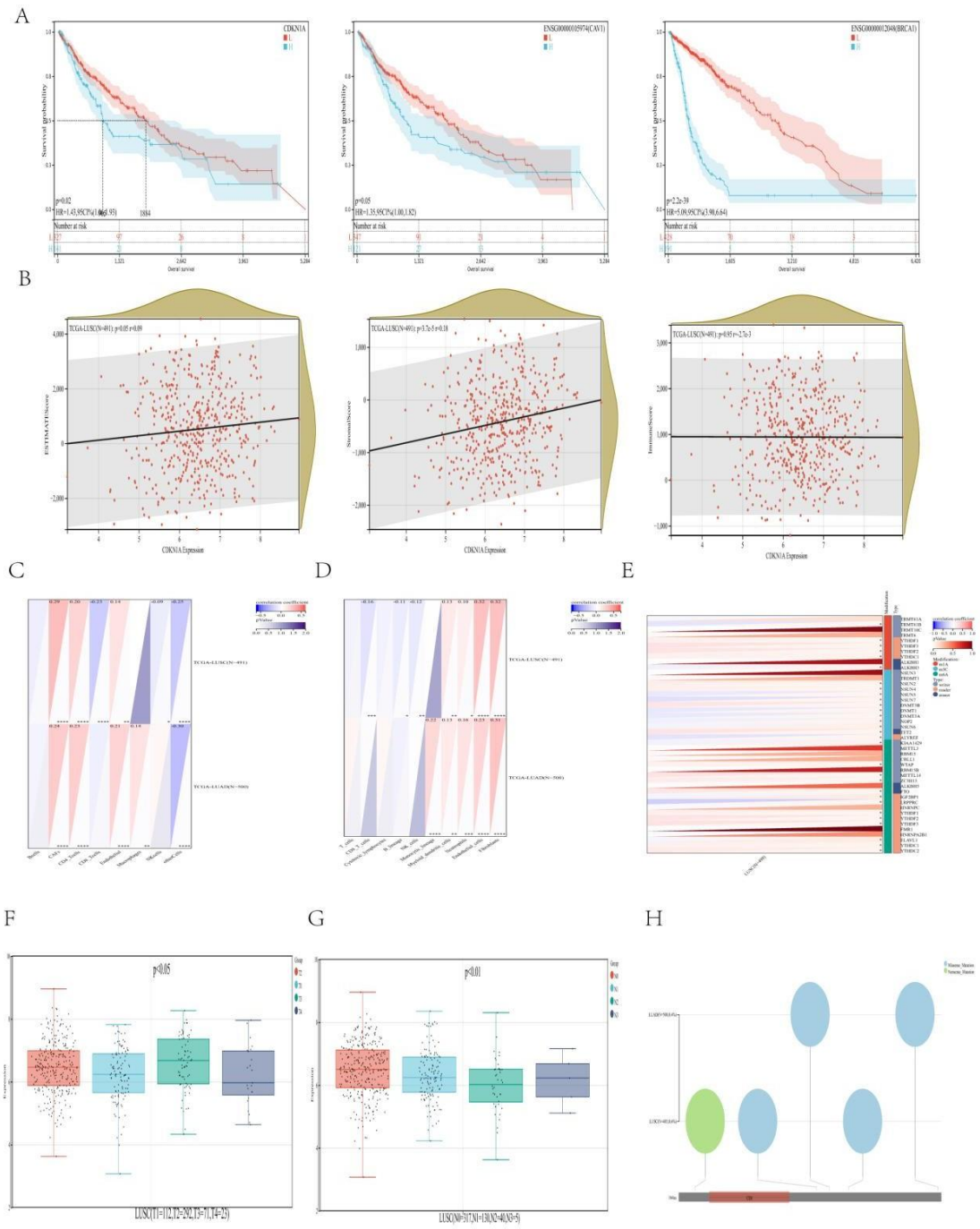

Figure 3: Prognostic and immune correlation analysis of core genes. (A) Prognostic analysis of core genes. (B) Correlation of CDKN1A with tumor microenvironment scores. (C, D) Correlation of CDKN1A with immune cells. (E, H) Epigenetic and SNP profile of CDKN1A in lung cancer patients. (F, G) Correlation of CDKN1A expression with clinical staging.

Research and exploration of Hub genes at the single cell level

We chose the dataset GSE117570 from the TISCH2 database, which was downscaled and grouped into 16 clusters **(Figure 4A).** UMAP plots highlight the primary cell kinds that are the center of attention, such as Malignant cells, Epithelial cells, epithelial cells, and so on **(Figure 4B)**, and bar and pie charts illustrate the cell

types and contents in 4 distinct patients, which helps to further investigate the tumor microenvironment of patients **(Figure 4C and D).** We further mapped our four Hub genes to single adult cell surfaces and investigated their differential expression in other cell populations, finding that CDKN1A was considerably differentially expressed in Th2, malignant, NK, and Plasma cells from different patients **(Figure 4I).** And it was expressed more in diverse cell types than the other genes **(Figure 4E-H).** Because CDKN1A is linked to the P53 pathway, we used GSEA to visualize the extent of enrichment of P53, DNA REPAIR, and other pathways at the single cell level **(Figure 5A).** The heat map depicts the relationship between various cellular taxa. We chose malignant cells and epithelial cells for cellular communication analysis and transcription factor identification because the CDKN1A gene is significantly expressed in both. The eggshell and reciprocal network diagrams proved connection between these two cell classes **(Figure 5B),** and the heat map detailed the ligands and receptors of distinct epithelial cells with different cells, with APP-CD74 being the most prominent **(Figure 5C).** **(Figure 5D and E)** demonstrates the identification of transcription factors of epithelial C12 and malignant cell C0 cluster.

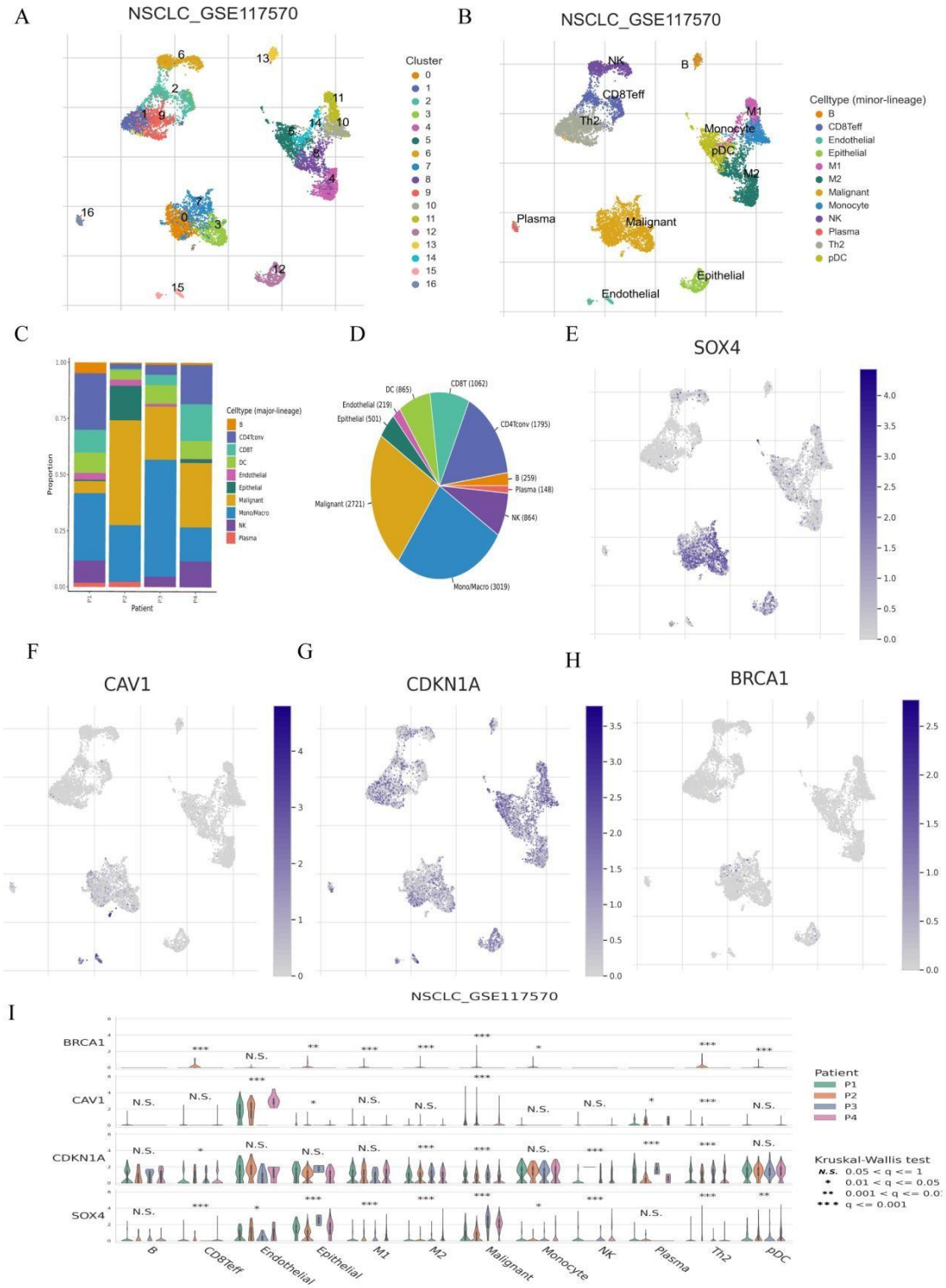

Figure 4: Exploration of core gene expression based on single cell level. (A, B) Reduced dimensional clustering and annotation of cell populations. (C, D) Statistical overview of cell composition of 4 patient samples. (E, F, G, H) Expression of CAV1, BRCA1, CDKN1A, SOX4 was demonstrated. (E, H) Epigenetic and SNP profile of CDKN1A in lung cancer patients. (I) Significance statistics of the differences of core genes in different samples.

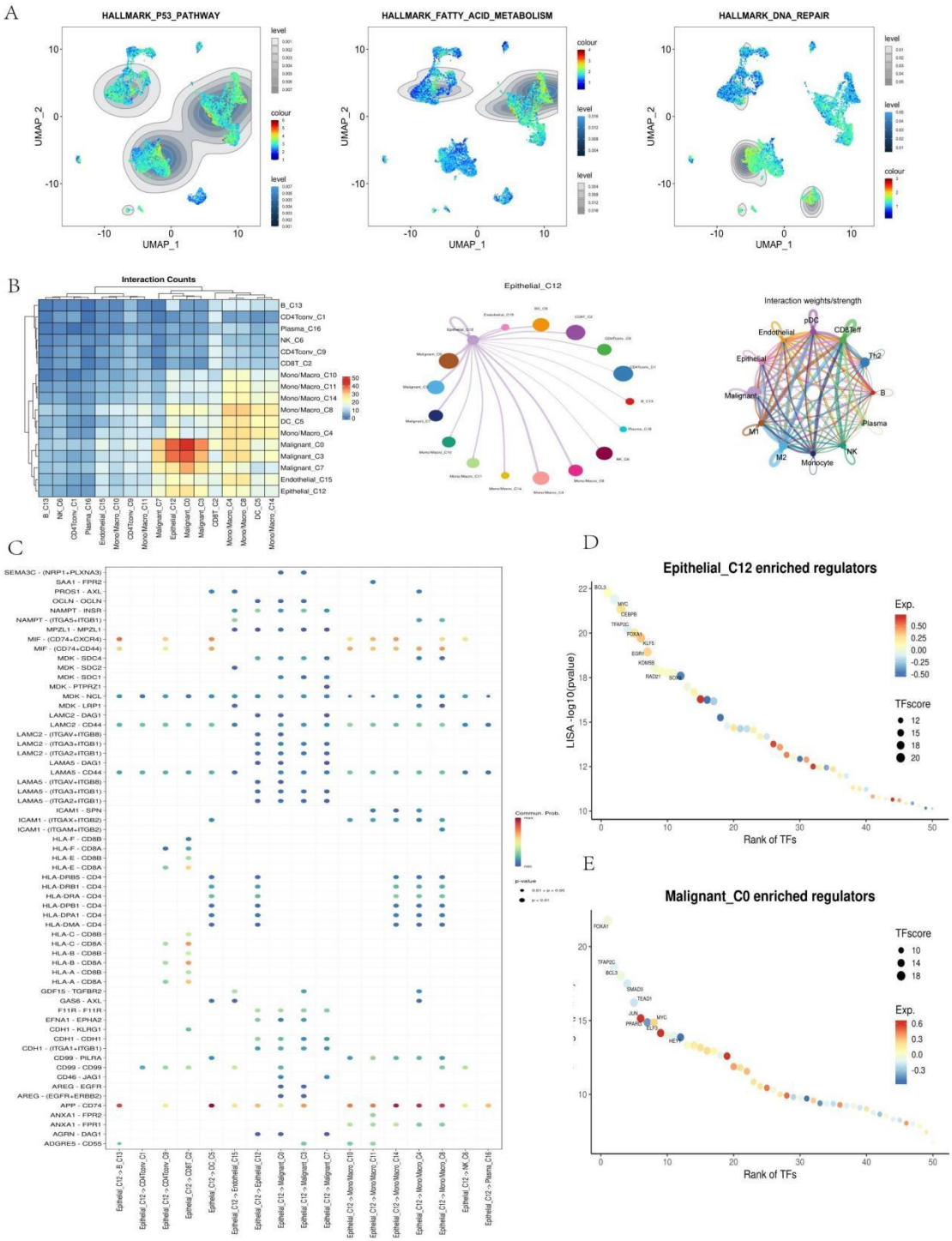

Figure 5: Cell Communication Analysis. (A) Visualization of disease-related pathways in single-cell datasets. (B) Analysis of the communication strength and correlation between different cell types demonstrated. (C) Ligand-receptor interactions between epithelial cells and different cells. (D, E) Identification of transcription factors in different cell subpopulations.

Analysis of the joint spatial transcriptome

We chose tissue sections from patients with non-small cell lung cancer and did a process analysis using the seurat program because the analysis of single cells lost the spatial dimensional analysis **(Figure 6A).** First, we checked the spatial transcriptome data for quality **(Figure 6B),** and then we visualized the four core genes in the

spatial dimension by descending the PCA, dividing the sectioned tissue into 12 subgroups **(Figure 6C),** and mapping the in-situ expression of genes onto the sections using the accompanying gene expression coordinates **(Figure 6D).** Among the MIA inference methods, the background genes of single cells and the background genes of the spatial transcriptome were examined using hypergeometric distribution, and then the cell type overlap of the spatial transcriptome was inferred, where the brown color in the red legend indicates enrichment (significantly high overlap); The blue color indicates depletion (significantly lower overlap), and the in situ expression of the combined previous genes shows that CDKN1A and SOX4, the majority of CAV1 are enriched in subpopulation 8,11, and the subpopulation and malignant and epithelial cells are highly overlapping, which to some extent validates our findings at the single cell level **(Figure 6E).** Finally, using the AddModuleScore function to score our genes as a set mapped to the spatial level, it can be seen that our gene set is higher in epithelial and malignant cells compared to other cells **(Figure 6F and G).**

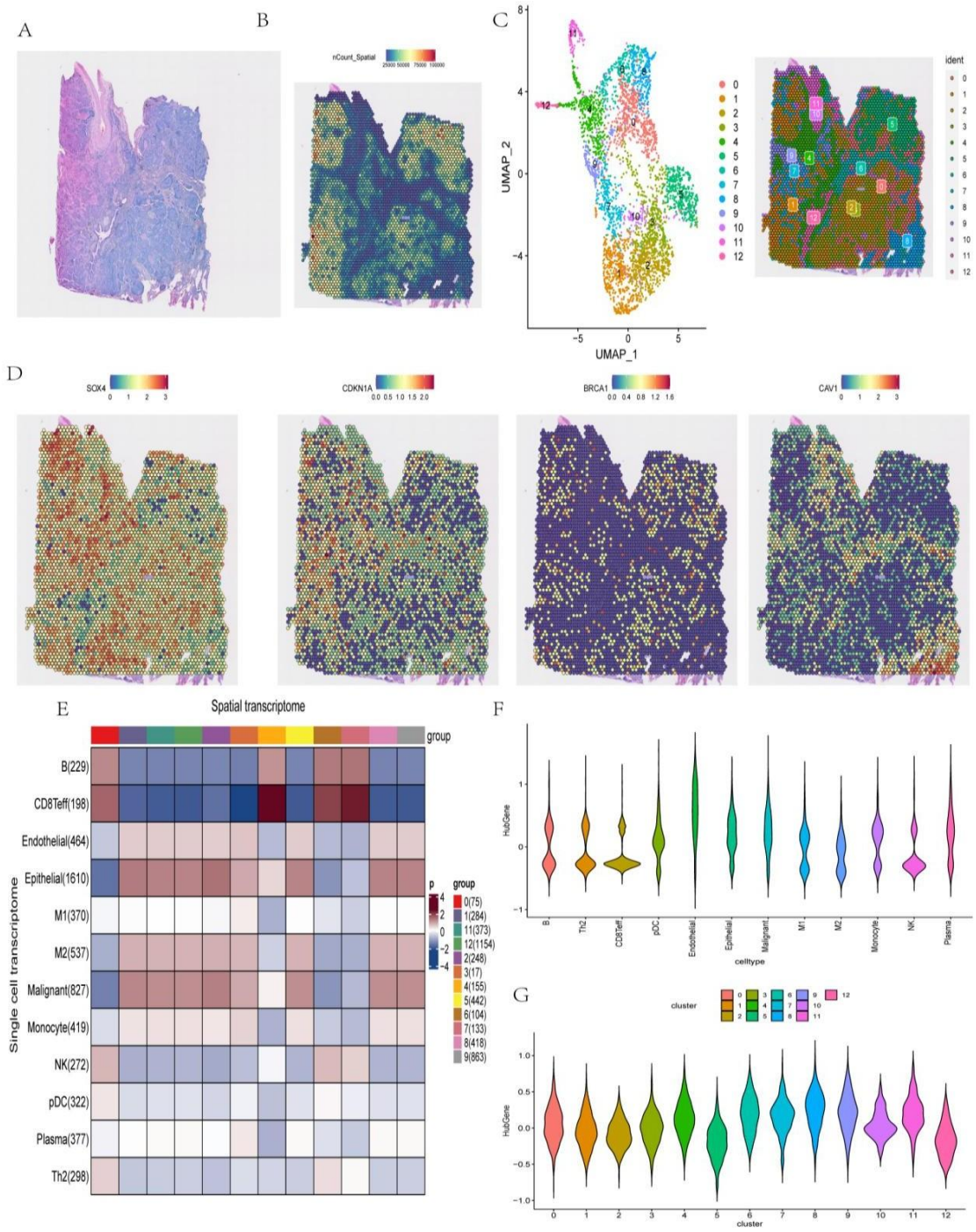

Figure 6: Exploring the expression of genes based on spatial transcriptome. (A) Histological section of a patient with squamous cell carcinoma of the lung. (B, C) Data quality control and dimensionality reduction clustering. (D) Spatial expression of hub genes. (E) Cell type inference for single cell transcriptome vs. spatial transcriptome. (F, G) Scores of Hub gene sets in different cell types and subpopulations.

Analysis of spatial datasets (image-based) and construction of ceRNA networks (competing endogenous RNAs)

The imaging images we utilized were generated by the Nanostring CosMx spatial molecular imager, and the descending clustering map of tissues is shown in **(Figure 7A and B)**. The basal cell populations are defined as tumor cells, which are seen to be spatially tightly organized, using the **Crop** () function. After zooming in, we

visualized the core genes, which can be found to be mostly located in the basal cells, i.e., tumor cells, which also validates the findings on single cell and spatially organized sections, respectively **(Figure 7C-E).** Finally, we constructed the lncRNA and miRNA regulatory networks associated with the core genes based on the prediction results of database spongeScan, TargetScan, miRDB, etc. after visualization by Cytoscape **(Figure 8).**

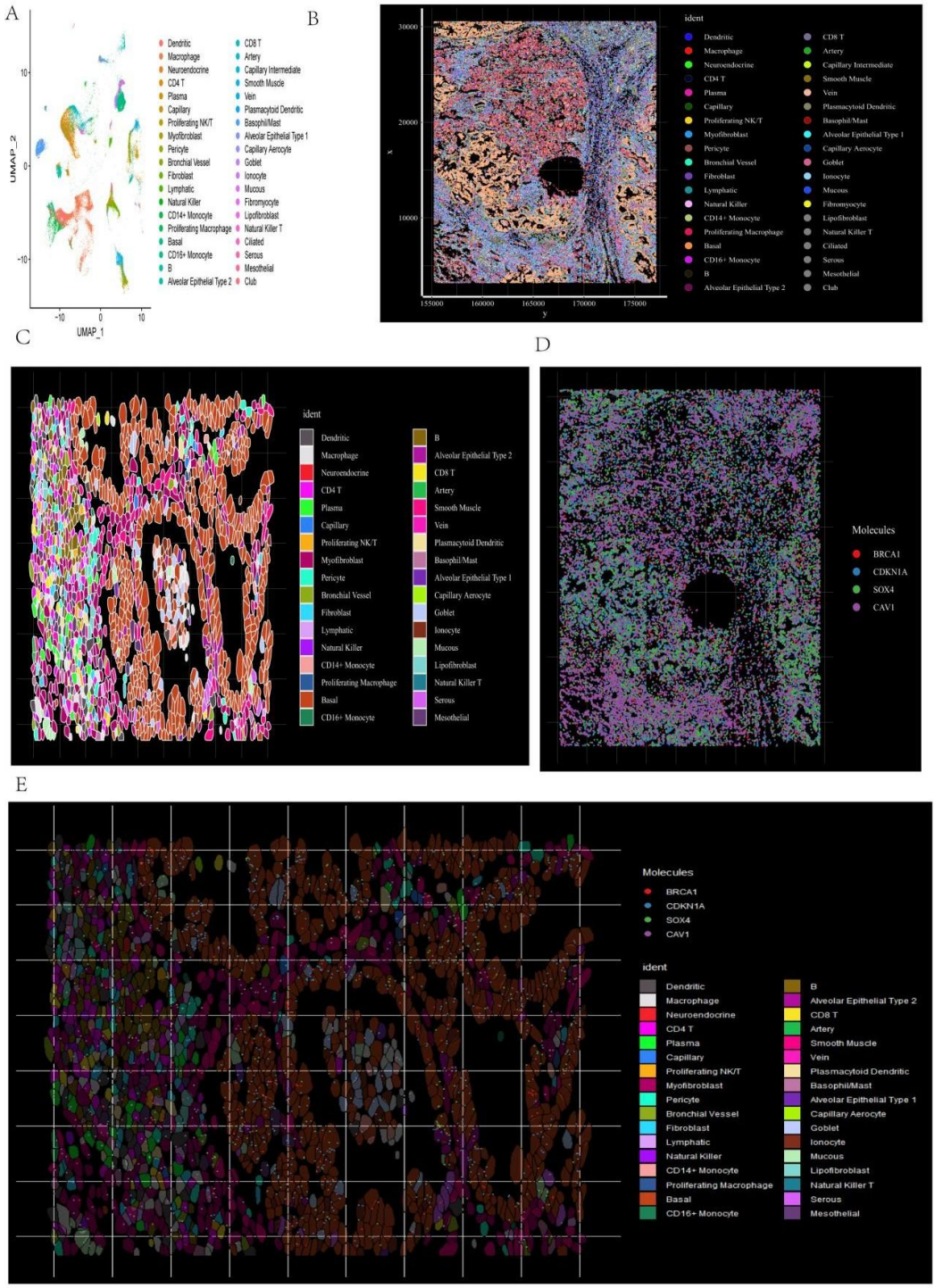

Figure 7: Exploration of hub gene expression based on spatial imaging images. (A, B) Cell type annotation and subgrouping of imaging images. (C, D, E) The expression of Hub genes in different cells is shown.

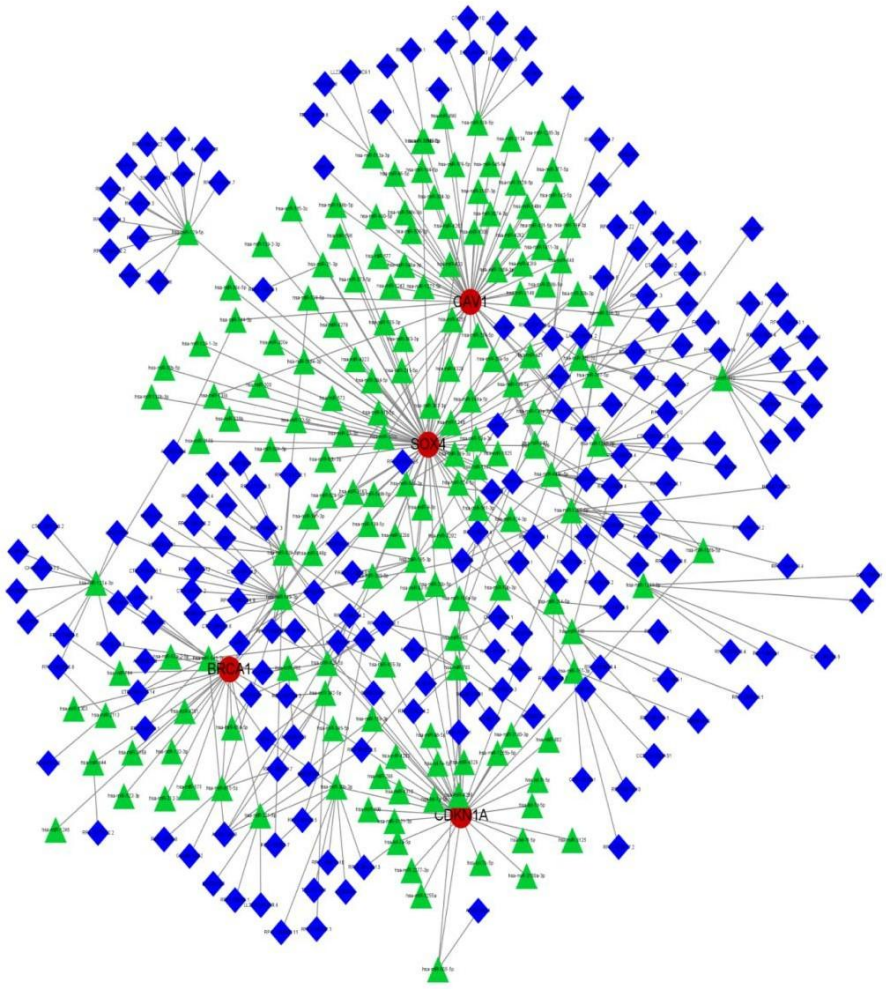

Figure 8: Building a ceRNA (miRNA-lncRNA-mRNA) regulatory network.

Discussion

With a prevalence of 13.48-31.79%, NAFLD is one of the most frequent liver diseases in individuals **[35].** NAFLD has been shown to cause an inflammatory infiltrate in which multiple T cell subsets are involved in NAFLD pathogenesis, and previous studies have found higher levels of CD4+ T and CD8+ T cell infiltration in peripheral blood in patients with non-alcoholic steatohepatitis **[7].** NAFLD has also been shown to disrupt the regional immune microenvironment, which may affect cancer progression. In NSCLC patients **[36],** hepatic steatosis is also seen as an independent predictor of liver metastases **[37].** In this study, we first identified genes that were differentially expressed in NAFLD and LUSC patients, and then used the WGCNA method to screen the most relevant modular genes for both diseases, yielding 11 shared genes that were not only differentially expressed in both datasets but also most relevant to the disease's phenotype. Our gene collection is closely related to the focal adhesion pathway, which has previously been linked to cancer aggressiveness, according to GO and KEGG analyses **[38].** We used protein interaction networks to identify the genes with the highest contribution between them CDKN1A, the tumor suppressor protein p53 tightly regulates the expression of this gene, which mediates a p53-dependent cell cycle G1 phase block in response to diverse stress stimuli. Recent research has revealed that CDKN1A is an autophagic fibroblast expression biomarker of senescence, and that it

plays an important role in the response to cisplatin-pemetrexed combinations in KRAS-mutated lung cancer cases, with a high potential biomarker value [39,40]. Furthermore, CDKN1A (p21) expression levels were significantly elevated in human NAFLD liver samples, and its involvement in the p53-mediated signaling pathway contributed to the progression of human NAFLD [41], as well as CDKN1A overexpression induced apoptosis and cell cycle arrest in lung cancer cells [42], where the CDKN1A SNP was associated with the development of hepatitis [43]. BRCA1 predicts clinical outcomes of chemotherapy in patients with non-small cell lung cancer [44]. CAV1 can be targeted by drugs in non-small cell lung cancer [45].

Based on bulk-RNA data, we performed a prognostic, clinical immune correlation analysis of CDKN1A. CDKN1A was positively correlated with stromal cells, T cells, which is consistent with previous studies. Each patient's tumor microenvironment is different, and finding a marker gene with a high confidence level is crucial, as it can improve the effectiveness of immunotherapy in patients. To further investigate whether our hub gene has a corresponding marker potential, we analyzed the gene expression values of CDKN1A in different cells in different samples by single cell sequencing. CDKN1A was significantly differentially expressed in Th2, M2 macrophages, and NK cells of the tumor microenvironment. and also, in malignant cells. We visualized the expression of P53, fatty acid metabolism, and DNA repair pathways in single cells to better understand the role of pathways associated with NAFLD in lung cancer patients, and we investigated the cellular communication between malignant cells and stromal cells with associated transcription factors, finding that the ligand receptor APP-CD74 was more relevant. We visualized our hub genes using the spatial transcriptome; the spatial location can help us better understand our in-situ expression in space; we inferred the cell type of the spatial transcriptome using the MIA approach; and we mapped the gene set scores to different cell types and clusters using the AddModuleScore scoring method; stromal and malignant cells scored higher, further validating our findings on top of single cells.

Finally, by constructing ceRNA regulatory networks, we can further understand the progression and regulation of our core genes on disease processes. Ferroptosis is a cell death caused by lipid peroxidation, and CDKN1A is wonderfully linked to the pathway of iron death. By promoting the expression of CDKN1A, P53 prevents iron death [46]. Previous studies have demonstrated that Ferroptosis is associated with the progression of NAFLD disease [47] and that Ferroptosis is closely associated with the development of non-small cell lung cancer. We therefore hypothesized that Ferroptosis as a process likely mediates disease progression in patients with both NAFLD and lung cancer, a conclusion that requires more in-depth ex vivo experiments to verify the plausibility.

Our study has several limitations, the first being that the very small dataset available for the association of liver fibrosis in NAFLD disease prevents us from validating our findings in more depth in NAFLD, and these results should subsequently be confirmed in depth in a larger study with a large sample size, and although we validated our in-situ expression in the spatial dimension, the hub gene and immune cell interactions are still worth investigating.

Conclusion

Our work identifies the function of shared genes CDKN1A, BRCA1, and CAV1 in squamous lung cancer, such as those between NAFLD and LUSC. In this investigation, new biomarkers for both were found.

References

1. Younossi Z, Tacke F, Arrese M, Chander Sharma B, Mostafa I, Bugianesi E, et al. Global Perspectives on Nonalcoholic Fatty Liver Disease and Nonalcoholic Steatohepatitis. Hepatology. 2019;69(6):2672-82.
2. Fan JG, Kim SU, Wong VW. New trends on obesity and NAFLD in Asia. J Hepatol. 2017;67(4):862-73.
3. Younossi Z, Anstee QM, Marietti M, Hardy T, Henry L, Eslam M, et al. Global burden of NAFLD and NASH: trends, predictions, risk factors and prevention. Nat Rev Gastroenterol Hepatol. 2018;15(1):11-20.
4. Younossi ZM, Koenig AB, Abdelatif D, Fazel Y, Henry L, Wymer M, et al. Global epidemiology of nonalcoholic fatty liver disease-Meta-analytic assessment of prevalence, incidence, and outcomes. Hepatology. 2016;64(1):73-84.
5. Fazel Y, Koenig AB, Sayiner M, Goodman ZD, Younossi ZM. Epidemiology and natural history of non-alcoholic fatty liver disease. Metabolism. 2016;65(8):1017-25.
6. McPherson S, Hardy T, Henderson E, Burt AD, Day CP, Anstee QM. Evidence of NAFLD progression from steatosis to fibrosing-steatohepatitis using paired biopsies: implications for prognosis and clinical management. J Hepatol. 2015;62(5):1148-55.
7. Inzaugarat ME, Ferreyra Solari NE, Billordo LA, Abecasis R, Gadano AC, Cherñavsky AC. Altered phenotype and functionality of circulating immune cells characterize adult patients with nonalcoholic steatohepatitis. J Clin Immunol. 2011;31(6):1120-30.
8. Chan WK, Treeprasertsuk S, Imajo K, Nakajima A, Seki Y, Kasama K, et al. Clinical features and treatment of nonalcoholic fatty liver disease across the Asia Pacific region-the GO ASIA initiative. Aliment Pharmacol Ther. 2018;47(6):816-25.
9. Angulo P, Kleiner DE, Dam-Larsen S, Adams LA, Bjornsson ES, Charatcharoenwitthaya P, et al. Liver Fibrosis, but No Other Histologic Features, Is Associated With Long-term Outcomes of Patients With Nonalcoholic Fatty Liver Disease. Gastroenterology. 2015;149(2):389-97.e10.
10. Ginsberg MS, Grewal RK, Heelan RT. Lung cancer. Radiol Clin North Am. 2007;45(1):21-43.
11. Janssen-Heijnen ML, Coebergh JW. The changing epidemiology of lung cancer in Europe. Lung Cancer. 2003;41(3):245-58.
12. Hirsch FR, Spreafico A, Novello S, Wood MD, Simms L, Papotti M. The prognostic and predictive role of histology in advanced non-small cell lung cancer: a literature review. J Thorac Oncol. 2008;3(12):1468-81.
13. Rosado-de-Christenson ML, Templeton PA, Moran CA. Bronchogenic carcinoma: radiologic-pathologic correlation. Radiographics. 1994;14(2):429-46; quiz 447-8.
14. Caliò A, Nottegar A, Gilioli E, Bria E, Pilotto S, Peretti U, et al. ALK/EML4 fusion gene may be found in pure squamous carcinoma of the lung. J Thorac Oncol. 2014;9(5):729-32.
15. König K, Peifer M, Fassunke J, Ihle MA, Künstlinger H, Heydt C, et al. Implementation of Amplicon Parallel Sequencing Leads to Improvement of Diagnosis and Therapy of Lung Cancer Patients. J J Thorac Oncol. 2015;10(7):1049-57.

16. Hanna N, Johnson D, Temin S, Baker S Jr, Brahmer J, Ellis PM, et al. Systemic Therapy for Stage IV Non-Small-Cell Lung Cancer: American Society of Clinical Oncology Clinical Practice Guideline Update. J Clin Oncol. 2017;35(30):3484-515.
17. Planchard D, Popat S, Kerr K, Novello S, Smit EF, Faivre-Finn C, et al. Metastatic non-small cell lung cancer: ESMO Clinical Practice Guidelines for diagnosis, treatment and follow-up. Ann Oncol. 2018;29(4):iv192-iv237.
18. Mantovani A, Petracca G, Beatrice G, Csermely A, Tilg H, Byrne CD, et al. Non-alcoholic fatty liver disease and increased risk of incident extrahepatic cancers: a meta-analysis of observational cohort studies. Gut. 2022;71(4):778-88.
19. Liu Z, Lin C, Suo C, Zhao R, Jin L, Zhang T, et al. Metabolic dysfunction-associated fatty liver disease and the risk of 24 specific cancers. Metabolism. 2022;127:154955.
20. Wang Z, Zhao X, Chen S, Wang Y, Cao L, Liao W, et al. Associations Between Nonalcoholic Fatty Liver Disease and Cancers in a Large Cohort in China. Clin Gastroenterol Hepatol. 2021;19(4):788-96.e4.
21. Lei Y, Tang R, Xu J, Wang W, Zhang B, Liu J, et al. Applications of single-cell sequencing in cancer research: progress and perspectives. J Hematol Oncol. 2021;14(1):91.
22. Zhang L, Chen D, Song D, Liu X, Zhang Y, Xu X, et al. Clinical and translational values of spatial transcriptomics. Signal Transduct Target Ther. 2022;7(1):111.
23. Love MI, Huber W, Anders S. Moderated estimation of fold change and dispersion for RNA-seq data with DESeq2. Genome Biol. 2014;15(12):550.
24. Ritchie ME, Phipson B, Wu D, Hu Y, Law CW, Shi W, et al. limma powers differential expression analyses for RNA-sequencing and microarray studies. Nucleic Acids Res. 2015;43(7):e47.
25. Langfelder P, Horvath S. WGCNA: an R package for weighted correlation network analysis. BMC Bioinformatics. 2008;9:559.
26. Shen Weitao, Song Ziguang, Zhong Xiao, Huang Mei, Shen Danting, Gao Pingping, et al. 2022. "Sangerbox: A Comprehensive, Interaction-Friendly Clinical Bioinformatics Analysis Platform." iMeta. 2022.
27. Bardou P, Mariette J, Escudié F, Djemiel C, Klopp C. jvenn: an interactive Venn diagram viewer. BMC Bioinformatics. 2014;15(1):293.
28. Wu T, Hu E, Xu S, Chen M, Guo P, Dai Z, et al. clusterProfiler 4.0: A universal enrichment tool for interpreting omics data. Innovation (Camb). 2021;2(3):100141.
29. Yoshihara K, Shahmoradgoli M, Martínez E, Vegesna R, Kim H, Torres-Garcia W, et al. Inferring tumour purity and stromal and immune cell admixture from expression data. Nat Commun. 2013;4:2612.
30. Racle J, Gfeller D. EPIC: A Tool to Estimate the Proportions of Different Cell Types from Bulk Gene Expression Data. Methods Mol Biol. 2020;2120:233-48.
31. Becht E, Giraldo NA, Lacroix L, Buttard B, Elarouci N, Petitprez F, et al. Estimating the population abundance of tissue-infiltrating immune and stromal cell populations using gene expression. Genome Biol. 2016;17(1):218.

32. Sun D, Wang J, Han Y, Dong X, Ge J, Zheng R, et al. TISCH: a comprehensive web resource enabling interactive single-cell transcriptome visualization of tumor microenvironment. Nucleic Acids Res. 2021;49(D1):D1420-D1430.
33. Hao Y, Hao S, Andersen-Nissen E, Mauck WM 3rd, Zheng S, Butler A, et al. Integrated analysis of multimodal single-cell data. Cell. 2021;184(13):3573-3587.e29.
34. Moncada R, Barkley D, Wagner F, Chiodin M, Devlin JC, Baron M, et al. Integrating microarray-based spatial transcriptomics and single-cell RNA-seq reveals tissue architecture in pancreatic ductal adenocarcinomas. Nat Biotechnol. 2020;38(3):333-42.
35. Valencia-Rodríguez A, Vera-Barajas A, Barranco-Fragoso B, Kúsulas-Delint D, Qi X, Méndez-Sánchez N. New insights into the association between non-alcoholic fatty liver disease and atherosclerosis. Ann Transl Med. 2019;7(8):S300.
36. Ma M, Duan R, Zhong H, Liang T, Guo L. The Crosstalk between Fat Homeostasis and Liver Regional Immunity in NAFLD. J Immunol Res. 2019;2019:3954890.
37. Wu W, Liao H, Ye W, Li X, Zhang J, Bu J. Fatty liver is a risk factor for liver metastasis in Chinese patients with non-small cell lung cancer. PeerJ. 2019;7:e6612.
38. Zhang H, Shao H, Golubovskaya VM, Chen H, Cance W, Adjei AA, et al. Efficacy of focal adhesion kinase inhibition in non-small cell lung cancer with oncogenically activated MAPK pathways. Br J Cancer. 2016;115(2):203-11.
39. Zamagni A, Pasini A, Pirini F, Ravaioli S, Giordano E, Tesei A, et al. CDKN1A upregulation and cisplatin - pemetrexed resistance in non - small cell lung cancer cells. Int J Oncol. 2020;56(6):1574-84.
40. Bernard M, Yang B, Migneault F, Turgeon J, Dieudé M, Olivier MA, et al. Autophagy drives fibroblast senescence through MTORC2 regulation. Autophagy. 2020;16(11):2004-16.
41. Tomita K, Teratani T, Suzuki T, Oshikawa T, Yokoyama H, Shimamura K, et al. p53/p66Shc-mediated signaling contributes to the progression of non-alcoholic steatohepatitis in humans and mice. J Hepatol. 2012;57(4):837-43.
42. Lee J, Kim K, Ryu TY, Jung CR, Lee MS, Lim JH, et al. EHMT1 knockdown induces apoptosis and cell cycle arrest in lung cancer cells by increasing CDKN1A expression. Mol Oncol. 2021;15(11):2989-3002.
43. Aravinthan A, Mells G, Allison M, Leathart J, Kotronen A, Yki-Jarvinen H, et al. Gene polymorphisms of cellular senescence marker p21 and disease progression in non-alcohol-related fatty liver disease. Cell Cycle. 2014;13(9):1489-94.
44. Yang Y, Xie Y, Xian L. Breast cancer susceptibility gene 1 (BRCA1) predict clinical outcome in platinum- and toxal-based chemotherapy in non-small-cell lung cancer (NSCLC) patients: a system review and meta-analysis. J Exp Clin Cancer Res. 2013;32(1):15.
45. Ali A, Levantini E, Fhu CW, Teo JT, Clohessy JG, Goggi JL, et al. CAV1 - GLUT3 signaling is important for cellular energy and can be targeted by Atorvastatin in Non-Small Cell Lung Cancer. Theranostics. 2019;9(21):6157-74.
46. Kang R, Kroemer G, Tang D. The tumor suppressor protein p53 and the ferroptosis network. Free Radic Biol Med. 2019;133:162-8.

47. Chen J, Li X, Ge C, Min J, Wang F. The multifaceted role of ferroptosis in liver disease. Cell Death Differ. 2022;29(3):467-80.

Citation of this Article

Yang H and Jiang QN. Integration of Spatial Transcriptome and Single-Cell Sequencing to Identify Specific Gene Expression in Spatially Organized Regions and Crosstalk between Tumor Microenvironments in Patients with Lung Squamous Cell Carcinoma Combined with Non-alcoholic Fatty Liver Disease. Mega J Case Rep. 2023; 6: 2001-2019.

Copyright

© 2023 Yang H. This is an open-access article distributed under the terms of the **Creative Commons Attribution License (CC BY).** The use, distribution or reproduction in other forums is permitted, provided the original author(s) or licensor are credited and that the original publication in this journal is cited, in accordance with accepted academic practice. No use, distribution or reproduction is permitted which does not comply with these terms.